A Covariance Matching-Based Adaptive Measurement Differencing Kalman Filter for INS's Error Compensation

CHINGIZ HAJIYEV[1], ULVIYE HACIZADE[2]
[1]Faculty of Aeronautics and Astronautics,
Istanbul Technical University,
Maslak, 34469, Istanbul,
TURKEY

[2]Department of Computer Engineering,
Halic University,
Güzeltepe Neighborhood, Temmuz Şehitler Street, No.15
34060 Eyüp-Istanbul,
TURKEY

Abstract: - In this study, a covariance matching-based adaptive measurement differencing Kalman filter (AMDKF) for the case of time-correlated measurement errors is proposed. The solution to the state estimation problem involves deriving a filter that accounts for measurement differences. Specifically, the measurement noise in the generated measurements is assumed to be correlated with the process noise. To address this issue in the context of correlated process and measurement noise, we propose an adaptive measurement differencing Kalman filter that is robust to measurement faults. We also evaluate the robustness of the suggested AMDKF through an analysis. When noise increment type sensor faults are present in the time-correlated inertial navigation systems (INS) measurements, the states of a multi-input/output aircraft model were estimated using both the previously developed measurement differencing Kalman filter (MDKF) and the suggested AMDKF and the results were compared.

Key-Words: - differencing Kalman filter, time-correlated error, process noise, adaptive Kalman filter, Inertial Navigation System, aircraft model.

Received: February 16, 2023. Revised: November 18, 2023. Accepted: December 3, 2023. Published: December 31, 2023.

1 Introduction

The primary sources of error in Inertial Navigation Systems (INS) are connected with insufficient initial knowledge and the gradual propagation of inaccuracies. The accelerometers' signals are integrated twice to determine location and velocity, in that order, subsequent to adjustments made for sensor error and gravity. The chief factors of velocity inaccuracies include the inexactness of accelerometer readings (generally due to bias and scale factors), slip-ups in local gravity calculation, and significant attitude inaccuracies resulting from gyroscope precession, [1].

Linear differential equations can characterize minor INS errors. Therefore, for the linear error analysis to remain reliable, the INS errors must remain small.

The accuracy of an INS's position and velocity estimates decays over time, [2]. The INS's drawbacks include its unbounded error growth. The use of more precise inertial sensors like accelerometers and gyroscopes can boost the INS's accuracy. However, there are reasonable boundaries to its performance. The cost of an inertial navigation system may be excessive.

Achieving high precision and low cost are fundamental considerations for numerous types of vehicles. This has been achieved in several works, [3], [4], [5], [6], [7], [8], [9], [10], [11], [12], [13], [14], [15], through the utilization of integrated navigation systems that combine inertial navigation systems with additional navigational aids. This allows for the comparison of independent measurements from external sensors that produce comparable values with the output of the INS. The discrepancies measured between multiple navigation systems are used to correct the inertial navigation system.

Inexpensive sensors, known for their low precision, have been the focus of research in this field for the past two decades. Consequently, many

algorithms have been developed to mitigate errors in inertial sensors. These algorithms are founded on either a mathematical model designed for the self-damping of inertial sensor errors or the integration of inertial sensors with external information sources including GPS receivers, magnetometers, barometers, and more. The study, [5], proposes a specific approach for compensating gyroscope drift via a PI controller based on magnetometer data in addition to a method for compensating inaccuracies in the horizontal channel of the navigation system.

An approach to refine the performance of the vertical accelerometer through a specific aircraft manoeuvre was analyzed in, [10], to implement supplementary in-flight calibration measures. Based on simulation results, conducting the proposed calibration manoeuvre before capturing the glide slope using a standalone INS feedback signal ensures satisfactory precision and safety standards (in the event of a barometric altimeter (BA) failure). Additionally, the suggested scheme for generating the measurement signal used in the Kalman filter allows for precise calibration of the vertical accelerometer without the requirement to estimate the BA bias. This confirms that the calibration accuracy is unaffected by the influence of BA bias.

The study, [11], proposes self-calibrated visual-inertial odometry (VIO), which applies a stereo camera and eliminates the need for calibration boards to estimate the intrinsic parameters of an inertial measurement unit (IMU), including scale factor and misalignment. Most visual-inertial navigation algorithms presume that the inertial and visual sensors are accurately calibrated. Nonetheless, modeling errors can impair navigation performance. To enhance the accuracy of the ego-motion modelling, we use an extended Kalman filter (EKF)-based pose estimator, with the addition of the IMU intrinsic parameter to the filter state. These variables are crucial to the effectiveness of ego-motion tracking since the intrinsic parameter is responsible for converting raw IMU readings.

There has been considerable debate surrounding the accuracy of estimating with a combined GPS and inertial navigation system using different types of Kalman filters. Because classical Kalman filters were incapable of withstanding noise and environmental disturbances, sensor fusion approaches employ adaptive and resilient structures. The study, [12], proposes numerous adaptable structures have been proposed in this context. The adaptation of the measurement covariance matrix, a factor for refining the process covariance matrix, and the Chi-square approach to identify and limit disturbances, are all beneficial to the fuzzy inference system.

External disturbances and imprecise noise statistics can cause non-Gaussian and unknown measurement noise to affect SINS/GPS integrated systems. To address this issue, a robust SINS/GPS integrated system based on the variational Bayesian method has been developed in, [13]. The unknown measurement noise covariance is initially estimated using the variational Bayesian-based Kalman filter. To mitigate non-Gaussian noise interference, the nonlinear robust filter is further enhanced by integrating the maximum correntropy criterion. Subsequently, the robust variational Bayesian approach leveraging the interacting multiple model is developed. This approach eliminates non-Gaussian noise interference to the measurement noise covariance estimation outcome.

In the study, [14], an integrated MEMS system is built that serves as a supporting system for the inertial navigation system and the Kalman filter when it comes to locating flying objects. The paper addresses the phenomena of unbalance in the INS system, as determined by an accelerometer, and summarizes the fundamentals of MEMS technology utilized in accelerometric measurements.

The study, [15], investigates the use of low-cost sensors, combining GNSS and IMU, as well as the impact of GNSS signal errors and different fusion algorithm designs. In order to enhance the accuracy and reliability of GNSS and IMU sensors for localization purposes, this paper introduces a segmented Rau-Tung-Striebel (RTS) smoothing algorithm and an error state extended Kalman filter algorithm. These technologies enable the INS to overcome the accumulated error over time, in case the GNSS signal is disrupted. The proposed method surpasses the traditional EKF algorithm in localization accuracy and linearity as revealed by the simulation results. Moreover, it displays remarkable robustness to achieve improved precision even in unfavorable GPS signal conditions.

To address the attitude of robots with high precision while employing a low-cost inertial measurement unit, calibration methods, and an attitude fusion filter were developed in, [16], to make better use of measurement data from several sensors. This calibration procedure accurately calibrates the accelerometer, magnetometer, and gyroscope.

The paper, [17], describes a method for self-calibrating IMUs using distributed sensor topologies. The IMU is made up of modules that are arranged along the measurement axes. A single-axis

gyroscope and three-axis accelerometer sensors are included in each module. Each module has its signal-conditioning circuits and processors. This enables the module to be calibrated on a single axis using a servo system based on a piezoelectric actuator. To calibrate the gyroscope sensor and accelerometer, the servo system produces high angular velocity and tangential acceleration.
The disadvantages of the IMU calibration methods presented in, [16] and [17], are that these methods require auxiliary tools and equipment.

The study, [18], presents an inertial navigation system error compensation method for the condition of time-correlated measurement errors. The proposed measurement differencing Kalman filter (MDKF) uses a measurement differencing approach-based Kalman filter to handle correlated systems with measurement noise. Due to the consideration of measurement differences, measurement biases are compensated for in this filter. This allows INS to be utilized for extended periods during flight, enabling autonomous navigation for real-time applications without requiring external navigation sources.

In this study, an adaptive version of the MDKF proposed in, [18], is developed. A covariance matching-based adaptive measurement differencing Kalman filter (AMDKF) for the case of time-correlated measurement errors is proposed. The robustness properties of the proposed AMDKF are investigated. Measurement differencing Kalman filter and proposed AMDKF were applied to estimate the states of a multi-input /output aircraft model in the presence of noise increment type sensor faults in the time-correlated INS measurements, and the obtained results were compared.

2 Problem Statement

The mathematical models for system and measurement can be expressed as follows:

$$\mathbf{x}(k)=\mathbf{A}\mathbf{x}(k-1)+\mathbf{B}\mathbf{u}(k-1)+\mathbf{G}\mathbf{w}(k-1) \quad (1)$$

$$\mathbf{z}(k)=\mathbf{H}\mathbf{x}(k)+\mathbf{v}(k)+\boldsymbol{\lambda}(k) \quad (2)$$

where $\mathbf{x}(k)$ is the system's state vector, $\mathbf{A}$ is the system transition matrix, $\mathbf{B}$ is the control distribution matrix, $\mathbf{u}(k)$ is the control input vector, $\mathbf{w}(k)$ is the random system noise, $\mathbf{G}$ is the system noise transition matrix, $\mathbf{z}(k)$ is the measurement vector, $\mathbf{H}$ is the system measurement matrix, $\mathbf{v}(k)$ is the measurement noise vector, $\boldsymbol{\lambda}(k)$ is the time-correlated INS errors process.

It is assumed that the random vectors $\mathbf{w}(k)$ and $\mathbf{v}(k)$ are zero-mean Gaussian white noise. Their covariance matrices are expressed as follows:

$$\begin{aligned} E\left[\mathbf{w}(k)\mathbf{w}^T(j)\right]&=\mathbf{Q}_w(k)\delta(kj)\\ E\left[\mathbf{v}(k)\mathbf{v}^T(j)\right]&=\mathbf{Q}_v(k)\delta(kj)\\ E\left[\mathbf{w}(k)\mathbf{v}^T(j)\right]&=0 \end{aligned} \quad (3)$$

where $\delta(kj)$ is the Kronecker delta symbol.

The INS errors $\boldsymbol{\lambda}(k)$ are correlated and considered to be, [19]:

$$\boldsymbol{\lambda}(k)=\mathbf{A}_n\boldsymbol{\lambda}(k-1)+\mathbf{B}_n\mathbf{U}(k-1) \quad (4)$$

where $\mathbf{A}_n$ and $\mathbf{B}_n$ are proper dimension matrices and $\mathbf{U}(j-1)$ is the Gaussian white noise vector with zero mean and covariance $\mathbf{Q}_U$:

$$E\left[\mathbf{U}(k)\right]=0;\ E\left[\mathbf{U}(k)\mathbf{U}^T(j)\right]=\mathbf{Q}_U(k)\delta(kj) \quad (5)$$

The equations (2) and (4) are unsuitable for state estimation of the system (1) via optimal discrete Kalman filter when time-correlated measurement noise is present. To address this problem, the optimal discrete Kalman filter should be adjusted.

3 The Measurement Differencing Kalman Filter

The measurement differencing approach is proposed as a means of developing a filter for estimating system states in the presence of time-correlated measurements (2). This technique utilizes a linear combination of measurements $\mathbf{z}(k+1)$ and $\mathbf{z}(k)$ as a system measurement, and excludes the correlated measurement errors $\boldsymbol{\lambda}(k)$. The appropriate linear combination is presented below, [1]:

$$\begin{aligned} \boldsymbol{\mu}(k)&=\mathbf{z}(k+1)-\mathbf{A}_n\mathbf{z}(k)=\left(\mathbf{H}\mathbf{A}-\mathbf{A}_n\mathbf{H}\right)\mathbf{x}(k)\\ &+\mathbf{H}\mathbf{B}\mathbf{u}(k)+\mathbf{H}\mathbf{G}\mathbf{w}(k)+\mathbf{B}_n\mathbf{U}(k)+\mathbf{v}(k+1)-\mathbf{A}_n\mathbf{v}(k) \end{aligned} \quad (6)$$

Instead of the correlated sequence $\boldsymbol{\lambda}(j)$, the measurement $\boldsymbol{\mu}(j)$ only includes the purely random sequence $\mathbf{HGw}(j)+\mathbf{B}_n\mathbf{U}(j)+\mathbf{v}(j+1)-\mathbf{A}_n\mathbf{v}(j)$. In this case, it is practical to formulate the state estimation problem in a structure that facilitates the application of the optimal discrete Kalman filter:

$$\begin{aligned}\mathbf{x}(j)&=\mathbf{Ax}(j-1)+\mathbf{Bu}(j-1)+\mathbf{Gw}(j-1)\\ \boldsymbol{\mu}(j-1)&=\mathbf{H}_d\mathbf{x}(j-1)+\mathbf{HBu}(j-1)+\boldsymbol{\xi}(j-1)\end{aligned} \tag{7}$$

where

$$\begin{aligned}\mathbf{H}_d&=\mathbf{HA}-\mathbf{A}_n\mathbf{H}\\ \boldsymbol{\mu}(k-1)&=\mathbf{z}(k)-\mathbf{A}_n\mathbf{z}(k-1)\\ \boldsymbol{\xi}(k-1)&=\mathbf{HGw}(k-1)+\\ &\mathbf{B}_n\mathbf{U}(k-1)+\mathbf{v}(k)-\mathbf{A}_n\mathbf{v}(k-1)\end{aligned} \tag{8}$$

It is shown in, [18], that the measurement noise $\boldsymbol{\xi}(k)$ in the system (7) is the purely random process (white noise) with an expected value:

$$\begin{aligned}&E\left[\boldsymbol{\xi}(k-1)\right]=\\ &E\left[\mathbf{HGw}(k-1)+\mathbf{B}_n\mathbf{U}(k-1)+\mathbf{v}(k)-\mathbf{A}_n\mathbf{v}(k-1)\right]=0\end{aligned} \tag{9}$$

and covariance

$$\begin{aligned}\mathbf{R}&=E\{\left[\mathbf{HGw}(k-1)+\mathbf{B}_n\mathbf{U}(k-1)+\mathbf{v}(k)-\mathbf{A}_n\mathbf{v}(k-1)\right]\\ &\times\left[\mathbf{HGw}(k-1)+\mathbf{B}_n\mathbf{U}(k-1)+\mathbf{v}(k)-\mathbf{A}_n\mathbf{v}(k-1)\right]^T\}\\ &=\mathbf{HGQ}_w\mathbf{G}^T\mathbf{H}^T+\mathbf{B}_n\mathbf{Q}_U\mathbf{B}_n^T+\mathbf{Q}_v+\mathbf{A}_n\mathbf{Q}_v\mathbf{A}_n^T\end{aligned} \tag{10}$$

As seen from the expressions (7) and (8), the process noise $\mathbf{Gw}(k-1)$ and the measurement noise $\boldsymbol{\xi}(k-1)$ are correlated:

$$\begin{aligned}&\mathbf{C}=E\left[\mathbf{Gw}(k-1)\boldsymbol{\xi}^T(k-1)\right]=\\ &E\left\{\mathbf{Gw}(k-1)\left[\mathbf{HGw}(k-1)+\mathbf{B}_n\mathbf{U}(k-1)+\mathbf{v}(k)-\mathbf{A}_n\mathbf{v}(k-1)\right]^T\right\}\\ &=E\left\{\mathbf{G}\left[\mathbf{w}(k-1)\mathbf{w}^T(k-1)\right]\mathbf{G}^T\mathbf{H}^T\right\}=\mathbf{GQ}_w\mathbf{G}^T\mathbf{H}^T\end{aligned} \tag{11}$$

Formula (7) shows that a known deterministic input $\mathbf{HBu}(j-1)$ is added to the output.

The measurement differencing Kalman filter (MDKF) formulas for estimation of the system (7) states are obtained in [18] in the following form.

The estimation equation of the MDKF

$$\begin{aligned}\hat{\mathbf{x}}(k/k)&=\hat{\mathbf{x}}(k/k-1)+\mathbf{K}(k)\times\\ &\{\boldsymbol{\mu}(k)-\mathbf{HBu}(k)-\mathbf{H}_d\hat{\mathbf{x}}(k/k-1)\}\end{aligned} \tag{12}$$

where $\hat{\mathbf{x}}(k/k-1)$ is the extrapolation value.

$$\hat{\mathbf{x}}(k/k-1)=\mathbf{A}\hat{\mathbf{x}}(k-1/k-1)+\mathbf{Bu}(k-1) \tag{13}$$

The optimal gain of the MDKF

$$\begin{aligned}&\mathbf{K}(k)=\left(\mathbf{P}(k/k-1)\mathbf{H}_d{}^T+\mathbf{C}(k)\right)\times\\ &\left[\mathbf{H}_d\mathbf{P}(k/k-1)\mathbf{H}_d{}^T+\mathbf{R}+\mathbf{H}_d\mathbf{C}(k)+\mathbf{C}(k)^T\mathbf{H}_d{}^T\right]^{-1}\end{aligned} \tag{14}$$

The extrapolation error covariance matrix

$$\mathbf{P}(k/k-1)=\mathbf{AP}(k-1/k-1)\mathbf{A}^T+\mathbf{GQ}_w\mathbf{G}^T. \tag{15}$$

The expression for the covariance matrix of estimation error $\mathbf{P}(k)$

$$\begin{aligned}&\mathbf{P}(k)=\mathbf{P}(k/k-1)-\mathbf{K}(k)\times\\ &\left[\mathbf{H}_d\mathbf{P}(k/k-1)\mathbf{H}_d^T+\mathbf{R}+\mathbf{H}_d\mathbf{C}(k)+\mathbf{C}(k)^T\mathbf{H}_d^T\right]\mathbf{K}(k)^T\end{aligned} \tag{16}$$

As seen from expressions (14) and (16), the gain matrix of MDKF $\mathbf{K}(k)$ and covariance matrix of estimation error $\mathbf{P}(k)$ involve the cross-correlation term $\mathbf{C}(k)$.

The measurement differencing Kalman filter for time-correlated measurement errors is represented by the formulas (10)-(16).

4 Adaptive Measurement Differencing Kalman Filter

A measurement noise covariance matching-based adaptive measurement differencing Kalman filter for the case of time-correlated measurement errors is presented below.

Statement 1: The measurement differencing Kalman filter (10)-(16) innovation sequence:

$$\boldsymbol{\Delta}(j)=\boldsymbol{\mu}(j)-\mathbf{HBu}(j)-\mathbf{H}_d\hat{\mathbf{x}}(j/j-1) \tag{17}$$

is a zero mean Gaussian random process with covariance:

$$E\left[\boldsymbol{\Delta}(j)\boldsymbol{\Delta}^T(k)\right]=\mathbf{H}_d\mathbf{P}(j/j-1)\mathbf{H}_d^T+\mathbf{R}+\mathbf{H}_d\mathbf{C}+\mathbf{C}^T\mathbf{H}_d^T \tag{18}$$

The proof of *Statement 1* is given in, [18].

An innovative sample covariance matrix:

$$\hat{\mathbf{S}}_{\Delta}(k)=\frac{1}{M}\sum_{j=k-M+1}^{k}\boldsymbol{\Delta}(j)\boldsymbol{\Delta}^{T}(j) \qquad (19)$$

will be used in the MDKF's R-adaptation technique. Here M is the number of implementations used (the width of the "sliding window").

The real and theoretical values of the MDKF innovation covariance can be compared to determine the multiple measurement noise scale factors (MMNSFs) for the R-adaptation. The multiple measurement noise scale matrix $\mathbf{S}(k)$ can be calculated from the equality of the real and theoretical innovation covariances as follows:

$$\frac{1}{M}\sum_{j=k-M+1}^{k}\left[\boldsymbol{\Delta}(j)\boldsymbol{\Delta}^{T}(j)\right]=\mathbf{H}_d\mathbf{P}(k/k-1)\mathbf{H}_d^{T} +\mathbf{S}(k)\mathbf{R}(k)+\mathbf{H}_d\mathbf{C}+\mathbf{C}^{T}\mathbf{H}_d^{T} \qquad (20)$$

$$\mathbf{S}(k)=\frac{\frac{1}{M}\sum_{j=k-M+1}^{k}\left[\boldsymbol{\Delta}(j)\boldsymbol{\Delta}^{T}(j)\right]-\mathbf{H}_d\mathbf{P}(k/k-1)\mathbf{H}_d^{T}-\mathbf{H}_d\mathbf{C}-\mathbf{C}^{T}\mathbf{H}_d^{T}}{\mathbf{R}(k)} \qquad (21)$$

However, due to the limited number of measurements M and the possibility of errors such as approximation errors and rounding errors in computer calculations, the matrix found by using (21) may not be diagonal and may contain diagonal elements that are "negative" or less than "one" (these are physically impossible). Thus, the following rule should be used when creating the scale matrix in order to avoid such a circumstance:

$$\mathbf{S}^{*}=diag\left(s_1^{*},s_2^{*},...,s_n^{*}\right), \qquad (22)$$

$$s_i^{*}=\max\left\{1,S_{ii}\right\} \qquad i=1,n. \qquad (23)$$

where S_{ii} is the i^{th} diagonal element of the matrix $\mathbf{S}$. In this way, in the case of measurement alfunction, $\mathbf{S}^{*}(k)$ will alter and have an impact on the Kalman gain:

$$\mathbf{K}(k)=\left(\mathbf{P}(k/k-1)\mathbf{H}_d{}^{T}+\mathbf{C}(k)\right)\times\left[\mathbf{H}_d\mathbf{P}(k/k-1)\mathbf{H}_d{}^{T}+\mathbf{S}^{*}(k)\mathbf{R}+\mathbf{H}_d\mathbf{C}(k)+\mathbf{C}(k)^{T}\mathbf{H}_d{}^{T}\right]^{-1} \qquad (24)$$

As a consequence of any form of malfunction, the relevant element of the scale matrix (which corresponds to the faulty measurement vector component) will increase. This subsequently reduces the Kalman gain, thereby minimizing the effect of innovation on the state update procedure and leading to greater accuracy of estimation results.

5 INS's Error Compensation using AMDKF

To compensate for INS time-correlated errors, the proposed adaptive measurement differencing Kalman filter is employed in a multi-input multi-output model for aircraft. The lateral and longitudinal motion of an aircraft is modeled using the state-space model based on, [20], which supplies information for the BRAVO - a twin-engine, jet fighter aircraft.

5.1 Simplified INS Error Model

This section outlines the semi-analytical error model for INS. Note that the INS error model as a whole poses a significant challenge. To simplify the model, certain assumptions can be made. For instance, in some scenarios, inter-channel connections can be disregarded. Therefore, to represent the INS error model, we used a simplified system of difference equations, as specified in, [3].

In the literature, [3], accelerometer errors and errors related to gravitational indetermination were classified as simple white noise inputs, random walk processes, first-order Gauss-Markov processes, and similar methods. This work utilizes the first-order Gauss-Markov process to model the INS errors, which are presented as follows:

$$\Delta a(j)=\Delta a(j-1)\left[1-\alpha_g\Delta t\right]+\Delta t U_{\Delta a}(j-1) \qquad (25)$$

$$\Delta g(j)=\Delta g(j-1)\left[1-\beta_g\Delta t\right]+\Delta t U_{\Delta g}(j-1) \qquad (26)$$

Here $\Delta a_x,\Delta a_y,\Delta a_z$ are the measurement errors of accelerometers, $\Delta g_x,\Delta g_y,\Delta g_z$ are the terms of error due to gravitational indetermination, Δt is the discretization interval, $U_{\Delta a}$ and $U_{\Delta g}$ are the white Gauss noises with zero mean; α_g and β_g are the terms for the correlation period.

5.2 Results of the AMDKF Simulation for the Error Compensation of the INS

The longitudinal and lateral dynamics of aircraft BRAVO have been examined through simulations. To estimate the aircraft's state vector, the presented in, [18], MDKF and proposed in this study AMDKF were employed.

Measurement noise increment type sensor faults

are simulated by multiplying the standard deviation of the pitch rate and pitch angle gyro measurement noises with a constant term in interval $80 \le k \le 150$

$$z_q(k) = z_q(k) + v_q(k) \times 8, \quad (80 \le k \le 150). \qquad (27)$$

$$z_\theta(k) = z_\theta(k) + v_\theta(k) \times 5, \quad (80 \le k \le 150). \qquad (28)$$

Figure 1, Figure 2, Figure 3, Figure 4, Figure 5, Figure 6, Figure 7 and Figure 8 show a subset of the simulation findings. Figure 1, Figure 3, Figure 5, Figure 7 demonstrate the estimation results for forward velocity (u), vertical velocity (w), pitch rate (q), and pitch angle (θ) when the presented AMDKF was employed. Figure 2, Figure 4, Figure 6, Figure 8 show the MDKF estimation results for the same aircraft states. The first section of Figure 1, Figure 2, Figure 3, Figure 4, Figure 5, Figure 6, Figure 7 and Figure 8 compares the estimation findings with actual values of the aircraft states. The error of the estimates is shown in the second half of the Figures. The state estimate errors are relatively minimal, as demonstrated by the graphs. The proposed adaptive measurement differencing Kalman filter allows the aircraft state vector to be estimated at each step while compensating for INS errors and noise increment type sensor faults.

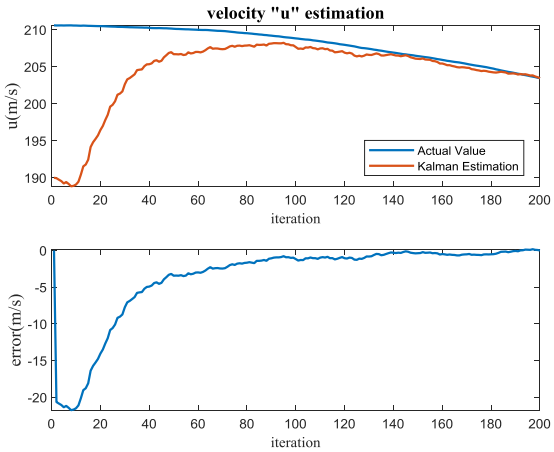

Fig. 1: AMDKF results for forward velocity estimation

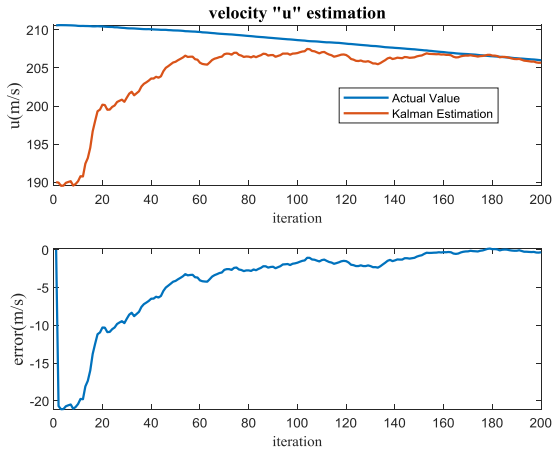

Fig. 2: MDKF results for forward velocity estimation

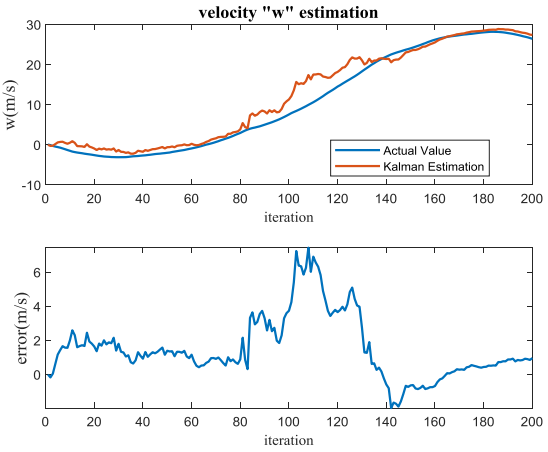

Fig. 3: AMDKF results for vertical velocity estimation

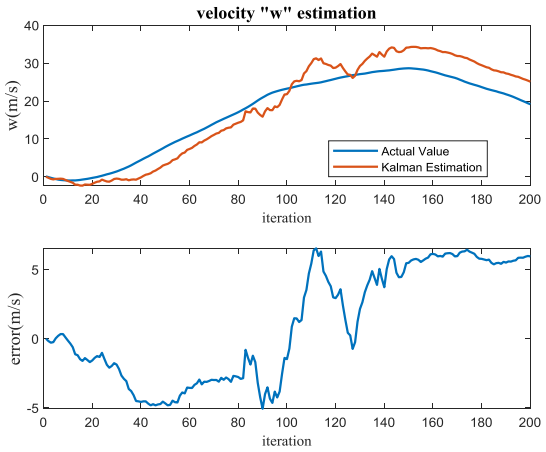

Fig. 4: MDKF results for vertical velocity estimation

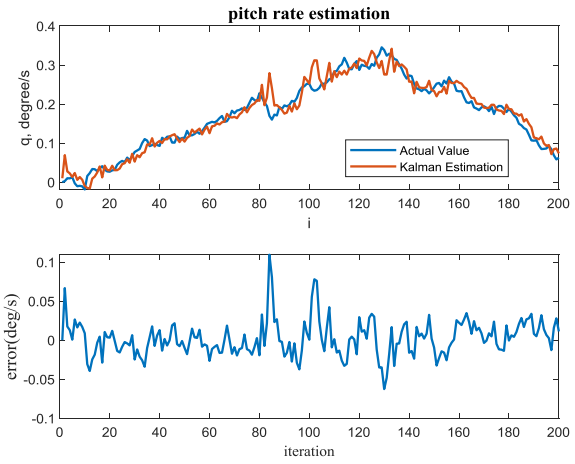

Fig. 5: AMDKF results for pitch rate estimation

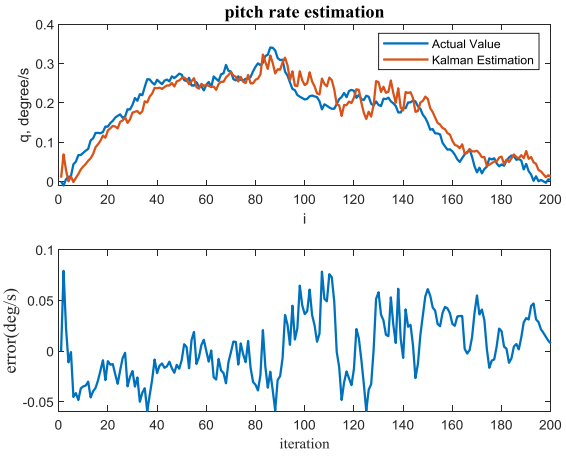

Fig. 6: MDKF results for pitch rate estimation

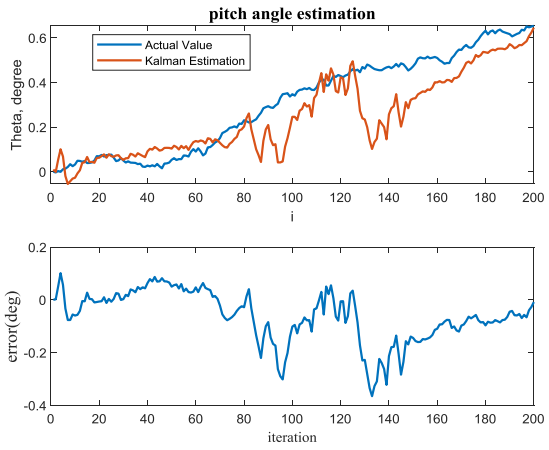

Fig. 7: AMDKF results for pitch angle estimation

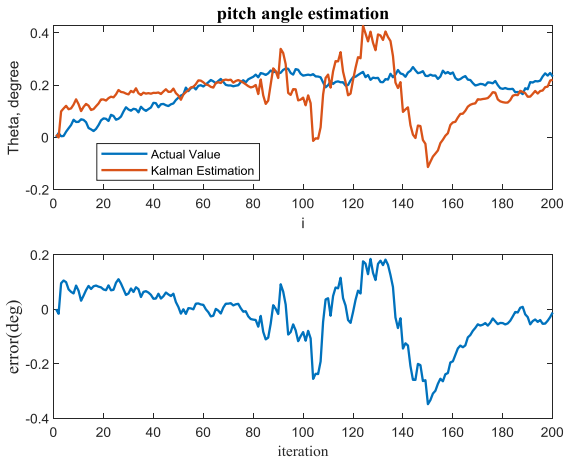

Fig. 8: MDKF results for pitch angle estimation

The Root Mean Square Errors (RMSE) of the estimation values, calculated between 80-150 iterations (after filter convergence), are likewise consistent with these findings. The following equation was used to calculate the RMSE values for the MDKF and AMDK estimates:

$$RMSE = \sqrt{\sum_{j=80}^{150} \frac{\left(\hat{x}(k/k) - x(k)\right)^2}{70}} \tag{29}$$

Table 1. RMSE of the state estimations in case of time-correlated bias and noise increment at INS measurements

RMSE	MDKF	AMDKF
u (m/s)	1.8245	0.9845
w (m/s)	3.8745	3.7517
q(deg/ s)	0.0379	0.0308
θ(deg)	0.1891	0.1229
β(deg)	0.0206	0.0234
p(deg/ s)	0.0360	0.0608
r(deg/ s)	0.0287	0.0303
ϕ(deg)	0.0743	0.0863

We can see that the suggested strategy improves estimation accuracy in the presence of noise increment type sensor faults.

In the presence of time-correlated bias and noise increment at INS measurements, the proposed AMDKF estimates for the longitudinal motion parameters outperform the simulation results in Table 1. For the lateral motion parameters, MDKF estimates are more accurate than AMDKF.

The proposed adaptive measurement differencing Kalman filter provides more accurate estimates for the faulty measurement channels in the presence of time-correlated INS's errors.

Furthermore, AMDKF estimation accuracy of the rest of longitudinal motion parameters, such as forward velocity (u) and vertical velocity (w), is better than MDKF, because these parameters are highly affected by faulty sensor data. This is because the suggested AMDKF compensates for INS errors as well as noise increment type sensor faults.

This research demonstrates that AMDKF is robust against noise increment type sensor faults. This is explained by the fact that the AMDKF measurement noise covariance rises as the scale matrix expression (21) is applied. As a result, the gain of AMDKF decreases and the weight of the measurements in the Kalman estimates is reduced, and the effect of the measurement result on the filter is less. The filter adapts to the noise increment type sensor fault. Table 1 displays the RMSE of the estimation values generated for the AMDKF and MDKF. As can be seen from Table 1, AMDKF is more accurate than MDKF for the faulty measurement channels and channels that are highly affected by faulty sensor data. Figure 1, Figure 2, Figure 3, Figure 4, Figure 5, Figure 6, Figure 7 and Figure 8 show that the proposed AMDKF provides accurate estimates of the aircraft's longitudinal states while being unaffected by INS measurement biases and noise increment type sensor faults. As a result, the INS can be used for extended periods in flight.

6 Conclusion

In this study, we present a covariance matching-based adaptive measurement differencing Kalman filter for time-correlated measurement errors and noise increment type sensor faults. Measurement differences are calculated in the filter to solve the state estimation problem. In this scenario, the measurement noise for the derived measurements is correlated with the process noise. AMDKF, robust to noise increment-type measurement faults is designed for correlated process and measurement noise situations. The developed AMDKF's robustness properties are studied. The proposed AMDKF and the previously developed MDKF were used to estimate the states of a multi-input/output aircraft model in the presence of noise increment type sensor faults in the time-correlated INS measurements and the results were compared.

Simulation results show that, in the presence of noise increment type sensor faults in the time-correlated INS measurements, AMDKF provides more accurate estimates for the faulty measurement channels and channels that are highly affected by faulty sensor data. The proposed AMDKF is robust to the time-correlated measurement errors and noise increment type sensor faults simultaneously.

Using only sensor error models, the proposed AMDKF can correct INS errors without a need for hardware redundancy. Thanks to this method, autonomous navigation is possible without the need for external navigation resources.

References:

[1] C. Hajiyev, "Measurement Differencing Approach Based Kalman Filter Applied to INS Error Compensation," *IFAC-PapersOnLine,* Vol. 49, No.17, 2016, pp. 343-348.

[2] A.V. Nebylov (Ed.), J. Watson (Ed.), "*Aerospace Navigation Systems*," John Wiley & Sons Inc, 2016.

[3] A.P. Zhukovskiy, V.V. Rastorguev, "*Complex Radio Navigation and Control Systems of Aircraft*," (In Russian), MAI, 1998.

[4] C.H. Eling, L. Klıngbeıl, H. Kuhlmann, "Real-Time Single-Frequency GPS/MEMS-IMU Attitude Determination of Lightweight UAVs," *Sensors*, Vol. 15, 2015, pp. 26212-26235.

[5] V. Sokolović, G. Dikić, G. Marković, R. Stančić, N. Lukić, "INS/GPS Navigation System Based on MEMS Technologies," *Strojniški vestnik - Journal of Mechanical Engineering*, Vol. 61, No. 7-8, 2015, pp.448-458. DOI: 10.5545/sv-jme.2014.2372.

[6] A.M. Kendre, V.N. Nitnaware, V.V. Thorat, "Low-Cost Tightly Coupled GPS/INS Integration Based on a Nonlinear Kalman Filtering Design," *Int. J. of Advanced Research in Computer and Communication Engineering*, Vol. 5, No.4, 2016, pp. 142-145.

[7] Z. Gao, D. Mu, Y. Zhong, C. Gu, "Constrained Unscented Particle Filter for SINS/GNSS/ADS Integrated Airship Navigation in the Presence of Wind Field Disturbance," *Sensors*, Vol.19, No.3, 2019, 471.

[8] D. Wang, X. Xu, Y.Yao, Y. Zhu, J.Tong, "A Hybrid Approach Based on Improved AR Model and MAA for INS/DVL Integrated Navigation Systems," *IEEE Access*, Vol.7, 2019, pp. 82794-82808.

[9] R. Song, X. Chen, Y. Fang, H. Huang, "Integrated Navigation of GPS/INS Based on Fusion of Recursive Maximum Likelihood IMM and Square-Root Cubature Kalman

Filter," *ISA Transactions*, Vol. 105, 2020, pp. 387-395.

[10] M. Nguyen, V. Kostiukov, C. Tran, "Effect of an In-Flight Vertical Accelerometer Calibration on Landing Accuracy After Baro-Inertial System Failure," *Aviation*, Vol. 24, Iss. 2, 2020, pp. 80–89. https://doi.org/10.3846/aviation.2020.12424.

[11] J. H. Jung, S. Heo and C. G. Park, "Observability Analysis of IMU Intrinsic Parameters in Stereo Visual–Inertial Odometry," *IEEE Transactions on Instrumentation and Measurement*, Vol. 69, No. 10, 2020, pp. 7530-7541.

[12] D. Sabzevari, A. Chatraei, "INS/GPS Sensor Fusion Based on Adaptive Fuzzy EKF with Sensitivity to Disturbances," *IET Radar, Sonar& Navigation,* Vol. 15, Iss. 11, 2021, pp. 1535-1549. DOI: 10.1049/rsn2.12144.

[13] X. Liu, X. Liu, Y. Yang, Y. Guo, W. Zhang, "Robust Variational Bayesian Method-Based SINS/GPS Integrated System," *Measurement,* Vol. 193, 2022, 110893. https://doi.org/10.1016/j.measurement.2022.110893.

[14] L. Setlak, R. Kowalik, "MEMS Electromechanical Microsystem as a Support System for the Position Determining Process with the Use of the Inertial Navigation System INS and Kalman Filter," *WSEAS Transactions on Applied and Theoretical Mechanics*, Vol. 14, 2019, Art. #11, pp. 105-117.

[15] Y. Yin, J. Zhang, M. Guo, X. Ning, Y. Wang, and J. Lu, "Sensor Fusion of GNSS and IMU Data for Robust Localization via Smoothed Error State Kalman Filter," *Sensors,* Vol. 23, 2023,3676, https://doi.org/10.3390/s23073676.

[16] M. Dong, G. Yao, J. Li, L. Zhang, "Calibration of Low-Cost IMU's Inertial Sensors for Improved Attitude Estimation," *Journal of Intelligent & Robotic Systems,* Vol. 100, 2020, pp.1015–1029, https://doi.org/10.1007/s10846-020-01259-0.

[17] U. Guner and J. Dasdemir, "Novel Self-Calibration Method for IMU Using Distributed Inertial Sensors," *IEEE Sensors Journal*, Vol. 23, No. 2, 2023, pp. 1527-1540.

[18] C. Hajiyev, "INS's Error Compensation Via Measurement Differencing Kalman Filter," *IEEE Transactions on Instrumentation and Measurement,* Vol.71, 2022, Paper 8503408, DOI: 10.1109/TIM.2022.3188059.

[19] R.G. Brown, P.Y.C. Hwang, "*Introduction to Random Signals and Applied Kalman Filtering with Matlab Exercises and Solutions*," 3rd Edition, John Wiley & Sons, 1997.

[20] D. Mclean, "*Automatic Flight Control Systems*," Hertfordshire, Prentice Hall International, 1990.

Contribution of Individual Authors to the Creation of a Scientific Article (Ghostwriting Policy)

- Chingiz Hajiyev carried out the conceptualization, investigation, methodology, validation, writing - review & editing.
- Ulviye Hacizade has organized and executed the simulation, data curation, formal analysis.

Sources of Funding for Research Presented in a Scientific Article or Scientific Article Itself

No funding was received for conducting this study.

Conflict of Interest

The authors have no conflicts of interest to declare.